RSC Advances

PAPER

View Article Online
View Journal | View Issue

Cite this: *RSC Adv.*, 2015, **5**, 86784

Preparation and performance of antibacterial layer-by-layer polyelectrolyte nanofiltration membranes based on metal–ligand coordination interactions

Hongyan Zhen,[ab] Tingting Wang,[b] Rui Jia,[b] Baowei Su*[ab] and Congjie Gao[ab]

Received 3rd August 2015
Accepted 29th September 2015

DOI: 10.1039/c5ra15427h

www.rsc.org/advances

The coordination interaction between transition metal Cu^{2+} ions and polyelectrolyte (PE) ligands is studied to prepare $(PEI/PSS(Cu)_{1/2})_n$ layer-by-layer (LBL) self-assembly (SA) nanofiltration (NF) membranes with unique antibacterial properties. The coordination interaction mechanism has been clearly illustrated by X-ray photoelectron spectroscopy (XPS) analysis of the chemical composition of the active skin layer, and the result reveals that about one third of the Cu^{2+} ions are involved in the interaction. The prepared $(PEI/PSS(Cu)_{1/2})_5$ LBL membrane has relatively smooth surface morphology and good separation performance, with a permeation flux of 65 L m^{-2} h^{-1} and rejection of about 84% for SO_4^{2-} at 1.0 MPa. It has an excellent antibacterial rate up to 94.2%. The performance of the LBL membranes could be improved, after cross-linking by glutaraldehyde (GA). This kind of LBL NF membrane shows potential application in the separation of monovalent and divalent anions.

Introduction

Nanofiltration (NF) membranes have been widely used in water treatment applications owing to their unique charge and separation properties. There are many methods to prepare NF membranes, such as phase inversion, interfacial polymerization, chemical cross-linking, layer by layer (LBL) self-assembly (SA), and so on. LBL technology is distinguished by its simplicity, versatility, and efficiency, which allows easy control over the thickness and surface properties.[1,2] By alternating adsorption of oppositely charged polyelectrolytes (PEs), the LBL method has gained increasing attention in the field of membrane preparation.

Till now, most research on LBL membrane preparation has been focused on the electrostatic interaction between PEs with opposite charges, which was firstly proposed by G. Decher and coworkers in 1991.[3] Since then, research on electrostatic SA has been widely carried out, not only in the preparation of PE multilayer membranes such as NF membranes,[4] pervaporation (PV) membranes,[5] and ion exchange membranes,[6] *etc.*, but also in the application of biological molecular SA and in the preparation of inorganic membrane materials with special performance. Wang *et al.* used electrostatic interaction as the driving force to prepare a PDADMAC/PSS multilayer NF membrane based on a polysulfone substrate, and found that the prepared membrane had good separation performance.[7]

Alternating adsorption of polyanions and polycations results in stepwise growth of polymer membranes and leads to unique properties due to the electrostatic interaction between oppositely charged molecules. The nanostructure of the LBL membrane can be tuned by the composition and the characteristics of the individual PE constituents. Studies have demonstrated two main steps during the adsorption and deposition of PEs.[8] Firstly, PEs undergo fast immobilization through a few sites of their chain segment onto the substrate surface; secondly, the entire PE chain combines with the substrate matrix slowly but closely by adjusting the conformation of the PE segments. Owing to the slow second step, the PE deposition time was mostly selected as 10–20 min to achieve a complete deposition.

In addition to electrostatic interaction, metal–ligand coordination interaction, charge transfer interaction, hydrogen bonding, covalent function, and the synergistic interaction of the above effects can also be used as the driving force. The metal coordination interaction force is much stronger than the electrostatic force, and thus the former is expected to be more stable in water than the latter. The first investigation of using the coordination effect as a film-forming driving force was reported by Mallouk,[9] who prepared an alternating deposition multilayer film with Zr^{4+} and alkyl compounds containing phosphate groups through the coordination effect between metal ions and phosphate. Xiong and Zhang *et al.* applied the coordination effect between poly(4-vinyl pyridine) (P4VP) and Cd^{2+} *via* the LBL method and prepared a $PSS(Cd)_{1/2}$/P4VP multilayer membrane on PEI modified substrates of quartz, CaF_2 and

[a]*Key Laboratory of Marine Chemistry Theory and Technology (Ocean University of China), Ministry of Education, 238 Songling Road, Qingdao 266100, China. E-mail: subaowei@ouc.edu.cn; Fax: +86 532 66786371; Tel: +86 532 66786371*

[b]*College of Chemistry & Chemical Engineering, Ocean University of China, 238 Songling Road, Qingdao 266100, China*

silicon; then they put the SA membranes into a H_2S atmosphere for 30 min and obtained polymer-bound CdS hybrid polymer/semiconductor nanoparticles, and demonstrated by infrared spectroscopy that the driving force of this process was the coordination interaction between the pyridine group and cadmium ions.[10] South *et al.* prepared hydrogen-storage SA multilayer films *via* the coordination effect between PVP and compounds containing Pd(II), and they successfully controlled the nature of the multilayer film by variation of the deposition conditions, solution additives and the polymer molecular weight.[11] Greenstein *et al.* reported an accelerated SA procedure using volatilization under natural conditions to ensure excessive ligands on the substrate surface to combine with metal ions by coordination effect, and the whole process could be controlled within only one minute, hence the membrane preparation time could be greatly shortened.[12] Zhang *et al.* prepared $(PSS(Co)_{1/2}/P4VP)_2$/PEI/PAN multilayer films on planar and 3D PAN substrate surfaces, respectively, using as driving force the coordination interaction between Co^{2+} and P4VP pyridine groups.[13] The prepared $PSS(Co)_{1/2}$/P4VP multilayer had not only high dehydration performance for solvent–water mixtures, but also high rejection for divalent ions, which proved that it could be used as an NF membrane.

Compared with other driving forces, coordination interaction can introduce transition metal ions into the membrane matrix. A lot of metal–ligand complexes can be used for SA,[14,15] since transition metals account for nearly half of the periodic table of the elements. In addition, some transition metals have special properties, for example, both silver and copper have bactericidal performance, thus functional films can be prepared by coordination.[16,17]

In recent years, more and more research on the preparation of functional membranes with antimicrobial properties using silver or copper ions has been carried out.[18–20] Fang *et al.* prepared ($[PSS/PDADMAC]_3[PAS/PAH\text{-}Ag]_3PSS$) multilayer NF membranes using LBL technology and coordination interaction, and the prepared NF membrane showed excellent antibacterial properties and the rejection for negative divalent ions reached 93%.[21] Zhang *et al.* prepared a copper-plating carbon nanotube (CNT) film by ion beam assisted deposition (IBAD) and found that the prepared CNT film possessed excellent antibacterial properties.[22]

To improve the performance of NF membranes regarding higher requirements under more challenging separation systems, a type of novel LBL NF membrane with high flux, excellent stability and antibacterial properties was prepared in this work, using the LBL method with the coordination effect as the driving force. As PEI is a typical water-soluble polyamine macromolecule with many amino functional groups, it was selected as a type of polycationic electrolyte and an ideal polymer ligand for coordination with transition metal copper ions. The coordination mechanism was analyzed through peak fitting of the XPS spectrum. Then, the effects of pH and electrolyte concentration in the PE solutions on the formation of the LBL membranes, as well as on the membrane morphology and performance, were extensively investigated. Finally, the separation performance and the antibacterial performance of the LBL NF membranes were investigated in detail.

Experimental

Materials

Polyacrylonitrile (PAN, MWCO = 50 000 dalton (Da)) and polyether sulfone (PES, MWCO = 20 000 Da) ultrafiltration (UF) membranes were purchased from Sepro Co., Xiamen, China. Polyethylenimine (PEI, MW = 60 000 Da, 50 wt% in water) and polystyrene sulfonic acid sodium (PSS, MW = 70 000 Da, 30 wt% in water) were purchased from Sigma-Aldrich Co., USA. Nutrient broth (CM106) was obtained from Beijing Land Bridge Technology Co., Ltd. Nutrient agar, glutaraldehyde (GA), NaOH, NaCl, Na_2SO_4, $MgCl_2$, $MgSO_4$ and $CuCl_2$ were all analytical reagents (AR) and purchased from Sinopharm Chemical Reagent Co., Ltd.

Preparation of LBL membranes

A PEI solution containing NaCl, and a PSS solution containing $CuCl_2$ were prepared, respectively. PAN, hydrolyzed PAN (H-PAN) and PES UF membranes were used as substrates, respectively. The H-PAN substrate was obtained by immersing the PAN substrate in aqueous NaOH solution to hydrolyze the –CN group on the PAN substrate surface into –COONa, and followed by immersing the substrate in deionized (DI) water to convert the –COONa into –COOH groups.

Prior to SA, the substrate was soaked in DI water for two hours to remove any impurities on its surface. Then it was taken out and immersed in one kind of PE solution, followed by rinsing with DI water. Afterward, it was immersed in the other kind of PE solution, followed by a second rinsing step with DI water. The immersion time in each solution was kept at 15 min, and the rinsing time with DI water between each immersion was 5 min. The described procedure was repeated until the desired bilayer number was achieved.

Factors influencing LBL membrane performance, such as species of substrate membrane, deposition sequence of PEs, concentration of transition metal ions, number of bilayers, as well as pH of the PEI solution, were investigated.

The influence of transition metal Cu^{2+} concentration on the membrane filtration performance was conducted by preparing $(PEI/PSS(Cu)_{1/2})_5$ membranes using 0.4% PSS solution with different concentrations of Cu^{2+} (0, 0.2, 0.4, 0.6, 0.8 M), referred to as PSS/Cu-0, PSS/Cu-0.1, PSS/Cu-0.2, PSS/Cu-0.4, PSS/Cu-0.6, PSS/Cu-0.8, respectively.

The influence of pH on the membrane performance was examined out using five different pH values (4, 6, 8, 10, 12) of the PEI solution.

The influence of bilayer number on the performance of LBL membranes was investigated with five different bilayers (1, 2, 3, 4, 5) prepared using an anionic PE solution of 0.4 M $CuCl_2$ and 0.4% PSS, and a cationic PE solution of 0.5 M NaCl and 0.3% PEI.

Characterization

The membrane morphology. The cross-sectional and surface morphologies of the prepared LBL NF membranes were investigated using a scanning electron microscope (SEM, S-4800,

Hitachi Co., Japan). The cross-section was obtained after breaking the membranes in liquid nitrogen. Prior to the characterization, the SEM samples were sputter-coated with 5 nm of gold on the membrane surface. A magnification ratio of 50 000 and an accelerating voltage of 7.0 kV were used for the observation of the membrane surface, while for the cross-section observation, the magnification ratio was set as 100 000. Energy Dispersive X-ray Detection (EDX) was also carried out on the SEM (S-4800, Hitachi Co., Japan).

The two-dimensional (2D) and three-dimensional (3D) surface topographies of the prepared LBL NF membranes were visualized by atomic force microscopy (AFM, Nano-3D, Nikon Co., Japan). Quantitative analysis of the membrane surface roughness was conducted based on AFM scans of at least three different areas, and root mean square roughness (RMS) was calculated.

Surface hydrophilicity. Membrane surface hydrophilicity was analyzed by measuring the contact angle of the membrane surface using a Contact Angle Goniometer (DSA100, Kruss, Germany) at room temperature and $(30 \pm 2)\%$ relative humidity with the static sessile drop method. During the measurement, a drop of DI water was deposited onto the sample surface using a micropipette, and the contact angle was measured automatically by a video camera using drop shape analysis software. The contact angle of each sample was measured at least 5 times, depending on the available membrane surface. Average and standard deviations of the contact angle were calculated. All membrane samples were dried in a vacuum oven at 50 °C for 24 hours prior to measuring their contact angles.

X-Ray photoelectron spectroscopy (XPS) analysis. The coordination effect and the chemical environment of certain atoms were analyzed by XPS spectra according to ref. 13, 23 and 24. XPS measurement was carried out on a PHI-5000 VersaProbe (Japan) and AES PHI-670Xi Scanning Auger Nanoprobe (Japan). All binding energies were referenced to the neutral C1s peak at 284.8 eV to compensate for the surface charging effects. The chemical shifts of the binding energy of different elements were analyzed, and then the valence state of atoms and distribution state of electrons were determined. Peak areas were obtained from fitting overlapping peaks after resolving with background subtraction.

Antibacterial activity. The dilution plate coating method was used to examine the antibacterial properties of the prepared membrane. *Escherichia coli* was selected as indicator bacterium, and nutrient agar plates from a solution of agar were prepared. A drop of bacterial suspension solution after being cultured with the substrate or self-assembly membrane was coated on a nutrient agar plate uniformly. The plates were incubated further at 37 °C for 24 h, and then the numbers of resultant colonies were counted. The bacteriostatic rate (R_B) was calculated according to the following eqn (1):

$$R_B = \frac{B - C}{B} \times 100\% \quad (1)$$

where B and C are the colony numbers on the incubated nutrient agar plate relating to the substrate and the LBL membrane, respectively. Replicates were performed and average values of the bacteriostatic rates of the substrate and LBL membranes were used for discussion.

Filtration. The separation performance of the prepared LBL membranes was measured *via* water permeability and salt rejection for single salt solution of 2000 mg L^{-1} Na_2SO_4 or NaCl, respectively. A home-made cross-flow pressure filtration apparatus was used in the NF experiments. The membrane sample was housed in a stainless steel sink with an effective area of 28.3 cm^2. In order to avoid concentration polarization, the feed flow rate was set at 40 L h^{-1} to maintain the average membrane channel velocity at about 0.1 m s^{-1}. All tests were performed at 1.0 MPa and 25 °C. The rejection, R, and the permeate flux, J_V, were calculated using eqn (2) and (3):

$$R = \frac{C_F - C_P}{C_F} \times 100\% \quad (2)$$

$$J_V = \frac{V}{At} \quad (3)$$

where C_P and C_F are the solute concentrations in the permeate and the feed, respectively; V is the volume of the permeate during time interval t; and A is the effective membrane area.

Replicates were performed and average values for salt rejections of each procedure were used for discussion.

Membrane stability. Because of the hydrophilicity, a PE membrane in aqueous solution will swell, which can affect its performance. The stability of the prepared LBL $(PEI/PSS(Cu)_{1/2})_5$ membrane after immersion in DI water for 10 days was tested *via* their rejection.

Glutaraldehyde post-processing. Considering that the PEI molecule contains many amino functional groups, they can form crosslinking in the presence of a crosslinking agent such as GA. The prepared LBL NF membrane was further immersed in 1.0% GA aqueous solution for 60 min to create crosslinking of the uncoordinated amino groups.

Results and discussion

Mechanism analysis of the coordinative self-assembly process

Fig. 1 shows the XPS spectrum of the prepared LBL multilayer membrane and partial enlargement spectrum of N and Cu elements. The results indicated the existence of Cu element in the skin layer of the prepared LBL NF membrane, which was also proved by the EDX spectra (Fig. 2).

According to Fig. 1, in the N1s spectrum, the binding energy at 399.9 eV can be assigned to the nitrogen atom in the $NH(NH_2)$ groups,[25] and there was a chemical shift up to 401.7 eV. In addition, $Cu(II)2p_{3/2}$ showed a chemical shift from 934.5 eV to 932.7 eV.

The chemical shift in the XPS can be explained by the charge transfer and electrostatic effects.[26] Each electron has one or several certain binding energy levels which are due to the strong coulombic force of the atomic nucleus. In addition, the outer electrons have a shielding effect on the inner electrons. When the outer electron cloud density reduces, its shielding effect on the inner electrons weakens, which leads to an increase in the binding energy of the inner electrons. Conversely, an increase in

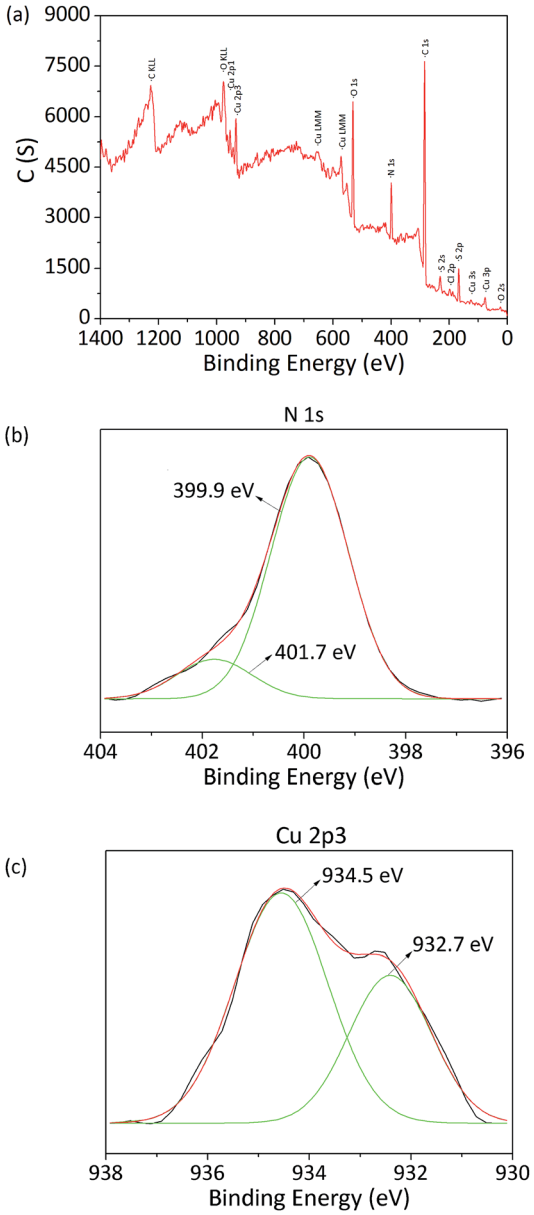

Fig. 1 The XPS spectrum of the prepared LBL $(PEI/PSS(Cu)_{1/2})_5$ membrane (a) and partial enlargement of the XPS spectrum of N (b) and Cu (c).

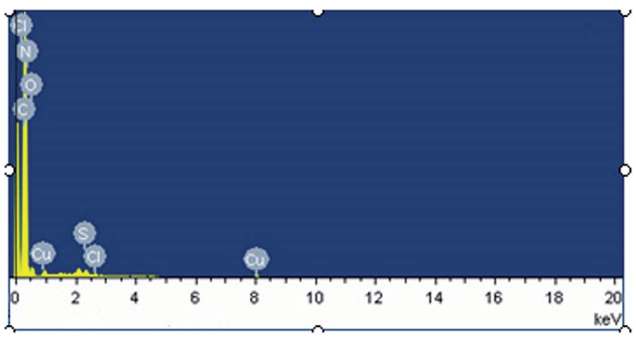

Fig. 2 EDX spectroscopy of the prepared LBL $(PEI/PSS(Cu)_{1/2})_5$ membrane.

the outer electron cloud density leads to a decrease in the inner electron binding energy.

PEI has a lot of amino *N* atoms on its linear macromolecular chain (the proportion of primary, secondary, tertiary amine is nearly 1 : 2 : 1), all the amines are located on the main chain and the branched chain can chelate with transition metal ions (Cu^{2+}, Ni^{2+}, Co^{2+}, Cd^{2+} *etc.*).[25,27–29] During the coordination interaction between the nitrogen groups of PEI and the Cu atom of $PSS(Cu)_{1/2}$, the electrons of the imine sites are drawn towards the copper ions, *i.e.* a pair of unpaired electrons on the N atom of the imine transfers to the empty orbitals of the Cu(II), causing a decrease in the N electron cloud density and an increase in the Cu(II) electron cloud density. Therefore, the binding energy of N1s increases and that of Cu(II) decreases. As shown in Fig. 1, during the SA process, the binding energy of a certain amount of N1s is shifted from 399.9 eV to 401.7 eV, and the binding energy of a certain amount of Cu(II) ions is shifted from 934.5 eV to 932.7 eV, which proves the occurrence of coordination interaction between the transition metal Cu^{2+} ion of $PSS(Cu_{1/2})$ and the N atom of PEI.[30]

In addition, according to the peak fitting data from Fig. 1(b), the peak areas of the binding energy at 399.9 eV and 401.7 eV for N1s were 1379.2 and 232.5, respectively, and the ratio of the areas was about 6 : 1. That is to say, about 14.25% of the N atoms had participated in the coordination reaction. Similarly, for Cu2p3, as shown in Fig. 1(c), the peak areas of the binding energy at 934.5 eV and 932.7 eV were 956.6 and 471.3, respectively, and the ratio of the areas was about 2 : 1. This means that about one third of the Cu(II) ions were involved in the coordination reaction. It can be seen from Table 1 that the relative atomic percentage of N1s and Cu2p3 in the prepared membrane were 11.6% and 1.6%, respectively. Thus the relative atomic percentages of N atoms and Cu(II) ions in the coordination complex were calculated to be 1.6% and 0.5% according to the molecular weight of each atoms, and the ratio was approximately 3 : 1. This is closely approaching the four-coordinate ratio, as it is well-known that Cu^{2+} forms stable complexes having a four-coordinate planar structure.[29,31]

Factors influencing LBL membrane performance

Substrate membrane and deposition sequence. The substrate membranes and the deposition sequences in the experiment are shown in Table 2. The variation in the rejection and the permeation flux of the SA membranes prepared with different substrates and deposition sequences with the increase of bilayer number were investigated, and the results are shown in Fig. 3.

It can be seen from Fig. 3 that the rejection of #1 PAN membranes remained essentially unchanged after depositing five bilayers, while that of #2 H-PAN membranes increased with the bilayer number. For #3 and #4 PES membranes, due to the uncharged property of the PES, the deposition of the first layer relied on the hydrophobic effect. When first depositing PSS, *i.e.* #3 membranes, the rejection was significantly higher than that of #4 membrane; however, the flux of #3 membrane was significantly lower than that of #4 membrane, which illustrated

Table 1 The relative atomic percentages and binding energy levels of elements based on XPS analysis

Element	C1s	N1s	O1s	S2p	Cu2p3	Cu LMM
Relative atomic percent (at%)	66.79	11.59	15.33	4.69	1.60	0.00
Binding energy (eV)	284.8	399.9, 401.7	531.3	167.7	932.7, 934.5	570.7, 572.4

Table 2 The substrate membranes and the deposition sequences in the experiment

Membrane no.	Substrate	MWCO (Dalton)	Deposition sequence
#1	PAN	50 000	PEI/PSS
#2	H-PAN	50 000	PEI/PSS
#3	PES	20 000	PSS/PEI
#4	PES	20 000	PEI/PSS

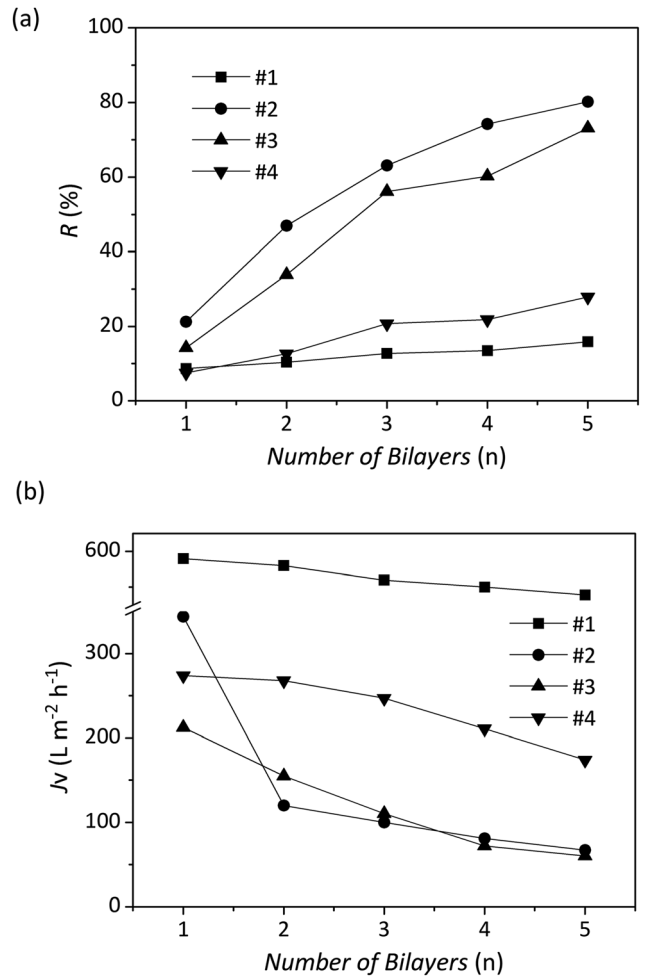

Fig. 3 The effect of number of bilayers ($n = 1$–5) on rejection (a) and flux (b) of the prepared LBL $(PEI/PSS(Cu)_{1/2})_n$ membranes with different substrates and deposition sequences.

that the deposition sequence of the first layer has a crucial influence on the membrane performance. The reason might be that when first depositing PSS, hydrophobic forces between the

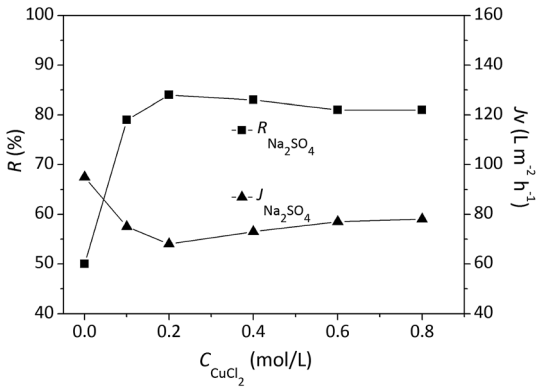

Fig. 4 The effect of transition metal concentration on rejection and flux of the prepared LBL $(PEI/PSS(Cu)_{1/2})_5$ membrane for Na_2SO_4 solution.

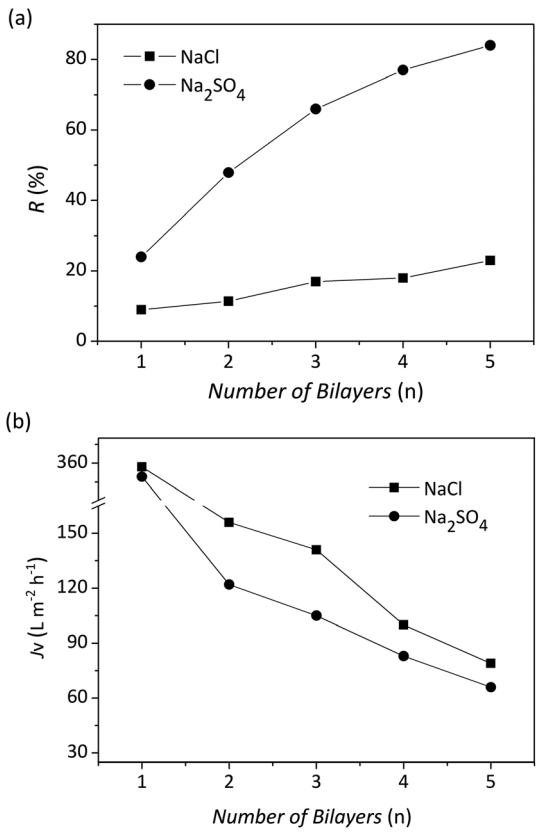

Fig. 5 The effect of number of bilayers ($n = 1$–5) on rejection (a) and flux (b) of the prepared LBL $(PEI/PSS(Cu)_{1/2})_n$ for Na_2SO_4 and NaCl solutions.

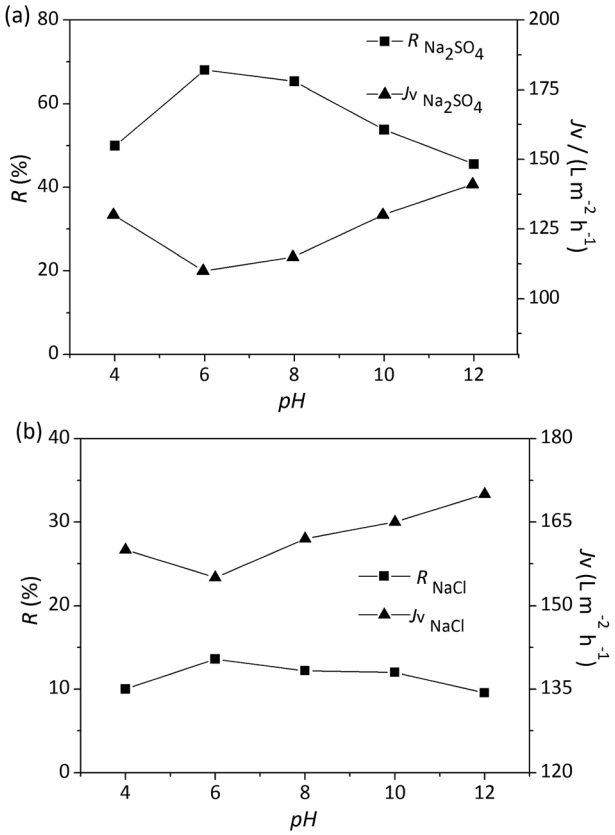

Fig. 6 The effect of pH on rejection and flux of the prepared LBL (PEI/$PSS(Cu)_{1/2})_3$ membrane for Na_2SO_4 (a) and NaCl (b) solutions.

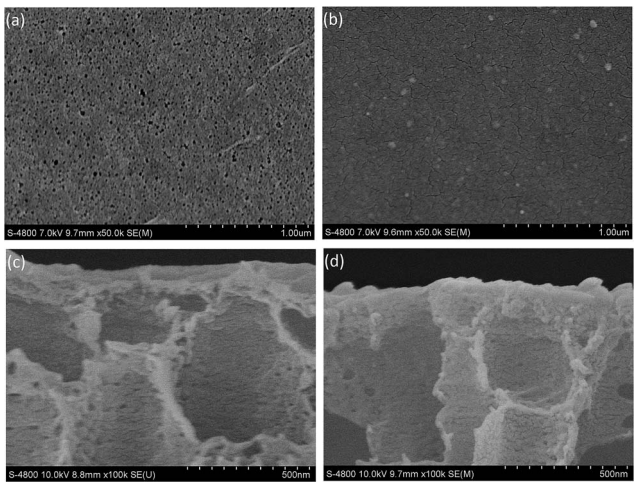

Fig. 7 SEM images of H-PAN substrate and the prepared LBL (PEI/$PSS(Cu)_{1/2})_5$ membrane (surface: substrate (a) and (PEI/$PSS(Cu)_{1/2})_5$ (b); cross-section: substrate (c) and (PEI/$PSS(Cu)_{1/2})_5$ (d)).

PES substrate membrane and PSS had an important effect on the later deposits.

As #2 membrane had essentially the same flux but relatively higher rejection compared with that of #3 membrane, we chose the H-PAN membrane as the substrate in the subsequent experiment, and as it was negatively charged, PEI was deposited first.

Concentration of transition metal. The effect of transition metal concentration on the separation performance of the prepared membrane is shown in Fig. 4.

PSS and PEI could combine with each other *via* electrostatic forces when there were no Cu^{2+} ions in the PSS solution; therefore, the prepared LBL membrane had some certain rejection. However, the counter-ion concentration in the PSS solution was low in this situation, and as the PSS segments were negatively charged, they were mutually repulsive, causing the extension of the polymer chains. Hence arrangement of the PSS molecules adsorbed on the substrate was not compact, and the following alternate deposition layer of PEs was not dense either, which resulted in a low rejection.

When adding Cu^{2+}, the membrane rejection to divalent ions showed a significant increasing trend as the concentration of Cu^{2+} increased up to 0.2 M, which clearly demonstrated the coordination effect of Cu^{2+}. However, when the concentration of Cu^{2+} increased above 0.2 M, the rejection then decreased slightly. This can be attributed to the aggregation effect of PEs at high concentration of Cu^{2+} ions, which caused the excessive deposition of a PSS mono-molecular layer and resulted in charge mismatch, eventually affecting the LBL process and the performance of the formed multilayer. Therefore, the optimal concentration of Cu^{2+} was 0.2–0.4 M.

The effect of number of bilayers on salt rejection. As shown in Fig. 5, the rejection for Na_2SO_4 appeared to show a tendency to increase and the flux presented a tendency to decrease as the bilayer number increased from 1 to 5. After deposition of five bilayers, the rejection for Na_2SO_4 was about 84% and the permeation flux was about 65 L m^{-2} h^{-1}; while the rejection for NaCl was 23% and the permeation flux was about 80 L m^{-2} h^{-1}.

pH of PEI solution. Fig. 6 gives the variation of rejection and permeate flux of the 3 bilayers LBL membrane prepared by varying pH of the PEI solutions.

It can be seen that the pH of the PEI solution influences the performance of the prepared LBL membranes. PEI is a weak polyelectrolyte, and compared with strong electrolytes, the charge density of weak electrolytes is strongly affected by the solution pH, and the degree of ionization of weak electrolytes in aqueous solution changes with the variation of pH. The charge density of PEs can affect their solution behavior and further affect the performance of the prepared membrane.[32] We can see from Fig. 6 that the rejection of both monovalent ions and divalent ions showed an increasing trend as the pH increased from 4 to 6, during which PEI ionization intensity increased. At pH 6, the PEI was strongly charged,[32] so that the prepared three-bilayer membrane had the highest rejection due to the stable adsorption of PE molecules. However, when the pH increased even higher, from 6 to 12, the charge density of PEI gradually decreased. Meanwhile, PSS was more soluble in an alkaline environment. Thus adsorption and desorption occurred simultaneously, which led to high permeability of the SA membrane.

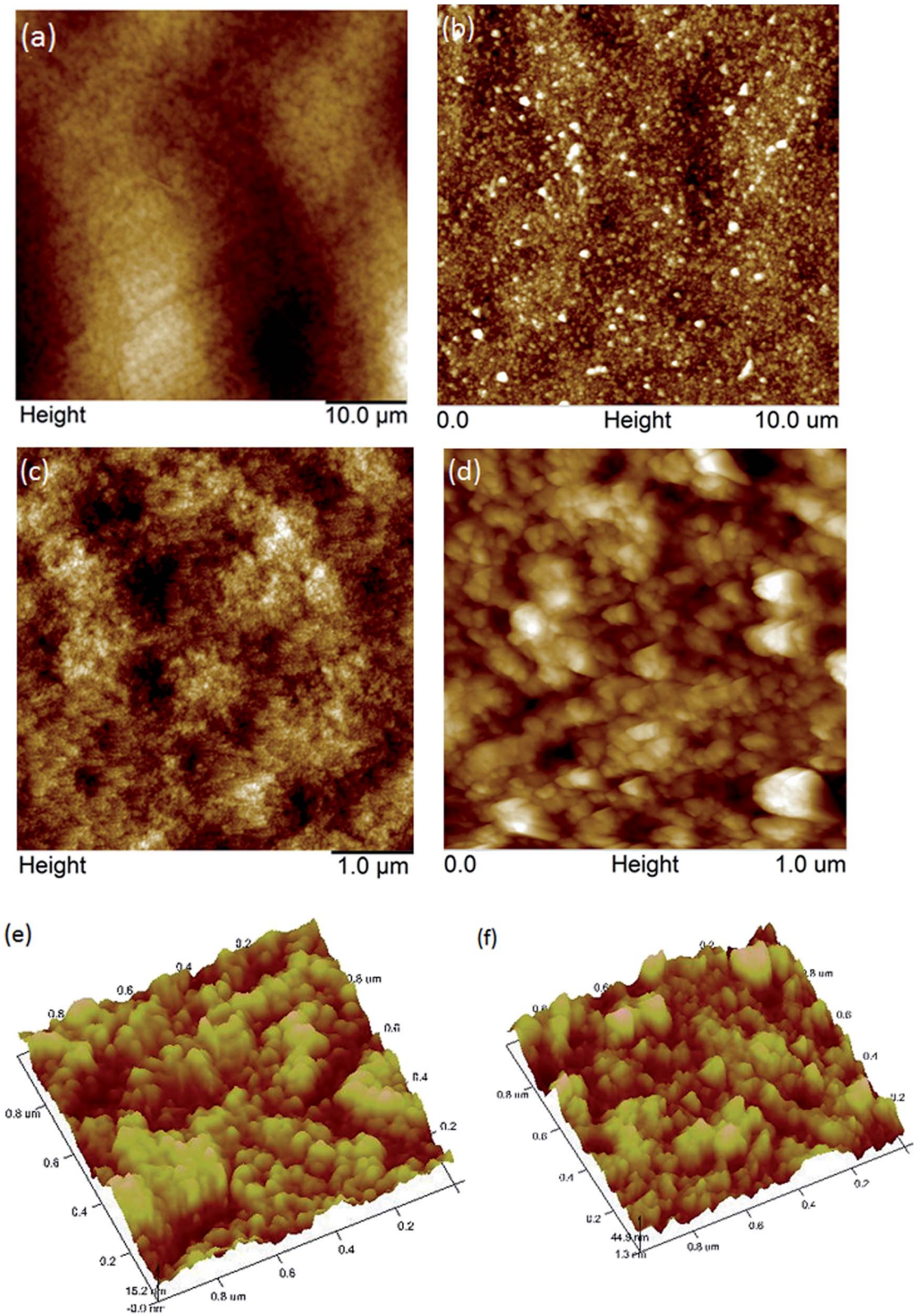

Fig. 8 AFM images of H-PAN substrate (2D images (a), (c) and 3D image (e)) and the prepared LBL (PEI/PSS(Cu)$_{1/2}$)$_5$ membrane (2D images (b), (d) and 3D image (f)).

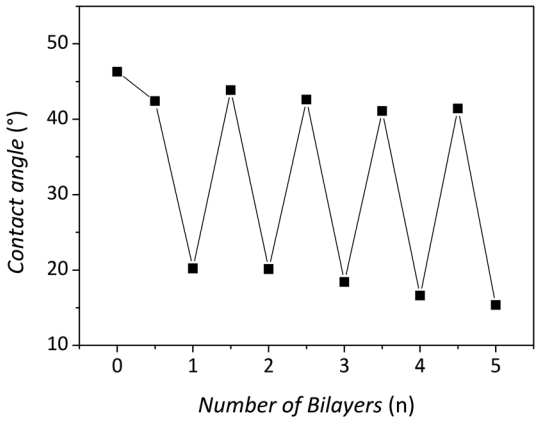

Fig. 9 The effect of number of bilayers ($n = 1$–5) on the contact angle of the LBL $(PEI/PSS(Cu)_{1/2})_n$ membrane ($n = 0$ referred to the H-PAN substrate).

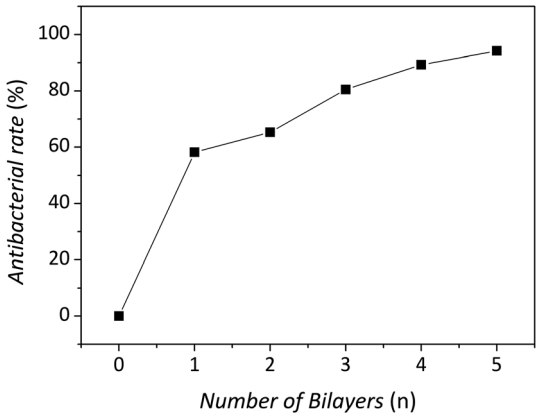

Fig. 11 The effect of number of bilayers ($n = 1$–5) on the antibacterial ratio of the LBL $(PEI/PSS(Cu)_{1/2})_n$ membranes ($n = 0$ refers to the H-PAN substrate).

Membrane morphology

Surface and cross-section morphology. The surface and cross-section morphologies of the H-PAN substrate and the LBL $(PEI/PSS(Cu)_{1/2})_5$ membrane are shown in Fig. 7. As can be seen from Fig. 7(a), many large pores, with size of about 10–20 nm, were found on the surface of the H-PAN substrate and they were relatively uniformly distributed. After static assembly of five bilayers, as shown in Fig. 7(b), the surface of $(PEI/PSS(Cu)_{1/2})_5$ became dense and the pores on the substrate surface had been covered completely, and no pores were visible. This in turn demonstrated that PEI and $PSS(Cu)_{1/2}$ were alternately assembled on the substrate surface successfully. Fig. 7(c) and (d) show the cross-sectional SEM images; compared with the H-PAN substrate, the thickness of the $(PEI/PSS(Cu)_{1/2})_5$ membrane increased slightly.

Table 3 The rejection and flux of the prepared LBL membrane for different kinds of salt solution (P: 1.0 MPa; T: 25 °C)

	Na_2SO_4	NaCl	$MgSO_4$	$MgCl_2$
R/%	84	23	65	19
J_V/L m^{-2} h^{-1}	65	80	75	78

Roughness. The 2D and 3D surface morphologies of the H-PAN substrate and the LBL $(PEI/PSS(Cu)_{1/2})_5$ membrane are shown in Fig. 8. It can be seen that the surface of the H-PAN substrate was relatively smooth, while that of the prepared LBL membrane after assembly showed an obviously increasing roughness. The RMS values of the H-PAN substrate, the prepared LBL $(PEI/PSS(Cu)_{1/2})_5$ membrane, and commercial DL

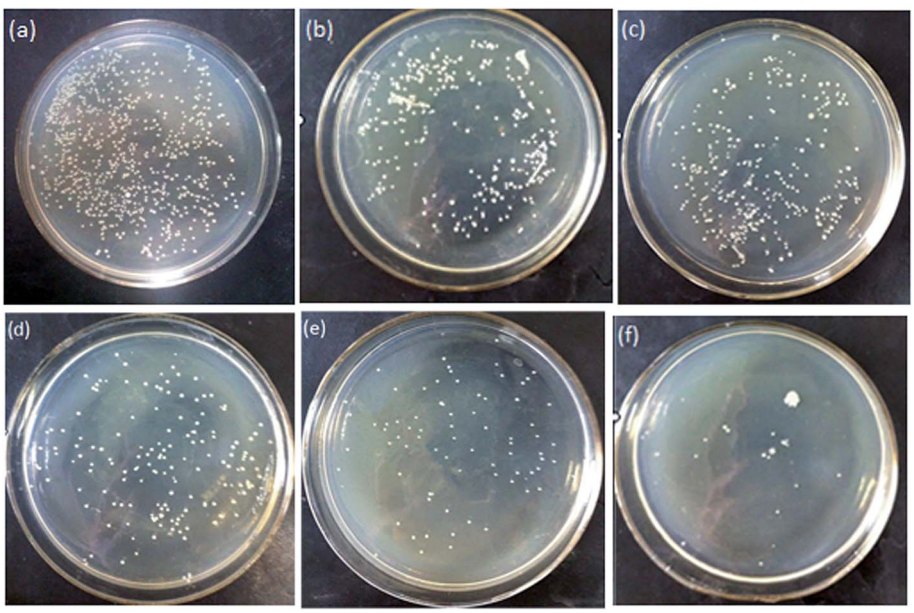

Fig. 10 Photos of antibacterial activity for the PAN substrate (a) and the LBL $(PEI/PSS(Cu)_{1/2})_n$ ($n = 1$–5) membranes (b–f).

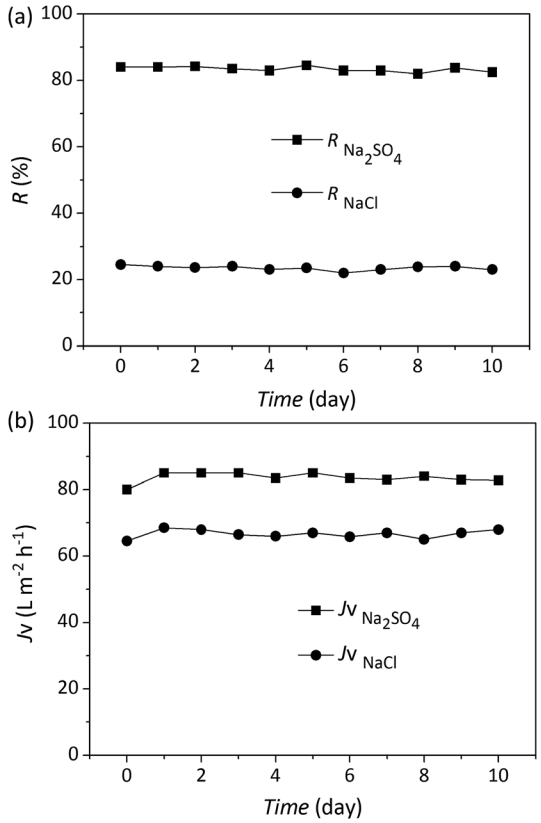

Fig. 12 Variation of rejection and flux of the prepared LBL (PEI/$PSS(Cu)_{1/2})_5$ membrane for Na_2SO_4 and NaCl solutions with immersion time.

Table 4 The rejection and flux of the prepared LBL membrane for Na_2SO_4 solution before and after GA crosslinking

Types of membrane	R/%	J_V/L m^{-2} h^{-1}
$(PEI/PSS(Cu)_{1/2})_5$	84	65
$(PEI/PSS(Cu)_{1/2})_5$/GA	90	53

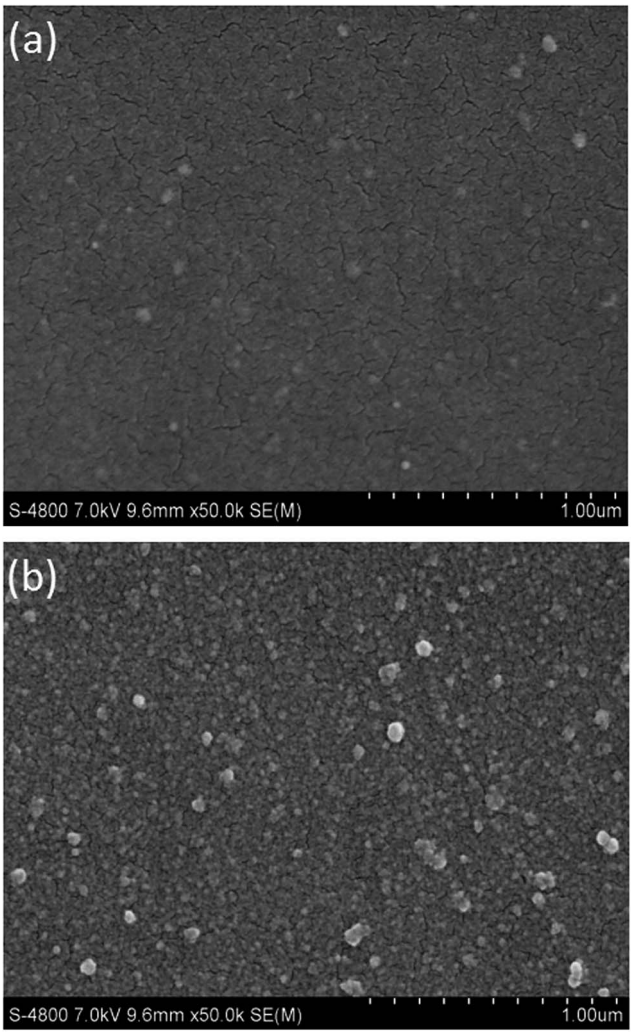

Fig. 13 The change in the membrane surface morphology before (a) and after (b) GA crosslinking.

membrane were about 3.59 nm, 9.68 nm, and 10.9 nm,[33] respectively. The surface roughness of the prepared LBL multilayer membrane is relatively close to that of the commercial DL membrane which has quite excellent anti-fouling performance. As membrane fouling is more easily formed on rough membranes than on smooth membranes,[34] the prepared LBL $(PEI/PSS(Cu)_{1/2})_5$ membrane might have excellent anti-fouling performance.

Surface hydrophilicity

The variation of contact angle with bilayer number is shown in Fig. 9.

It can be seen that the contact angle of the H-PAN substrate membrane was 46.3° (corresponding to the point of $n = 0$), and that of the unmodified PAN membrane was 60.7° (not shown in Fig. 9), which indicated that alkali modification could improve the hydrophilicity of the substrate. Subsequently, the SA process effectively changed the hydrophilicity of the membrane surface, and the contact angle varied alternately with the alternating deposition of the cationic and anionic PEs. When the outermost skin layer was the same kind of PE, the contact angle showed a decreasing tendency with the increase of the layer number of the same PE, which meant that the hydrophilicity became better. When the outermost layer was PSS, the contact angle of the LBL membrane was maintained at 15–20°; this is mainly due to the excellent hydrophilicity of PSS as a very strong hydrophilic surfactant. Therefore, the prepared LBL membrane had excellent hydrophilicity with the outermost deposition of $PSS(Cu)_{1/2}$ electrolyte solution.

Antibacterial ability

The antibacterial activity of the UF substrate and the LBL (PEI/$PSS(Cu)_{1/2})_n$ ($n = 1$–5) membranes is shown in Fig. 10. It can be seen from Fig. 10(a) that there were a large number of bacterial colonies on the nutritional agar medium surface of the

substrate. With the increase in the bilayer number, the colonies reduced significantly, as can be seen from Fig. 10(b)–(f), especially for the five-bilayer membrane (Fig. 10(f)) which had only a few sporadic colonies. This demonstrated that the prepared LBL membrane had good antibacterial ability.

The antibacterial efficiency was calculated and shown in Fig. 11. The larger the bilayer number, the better the antibacterial ability. For the five layers of LBL $(PEI/PSS(Cu)_{1/2})_5$ membrane, the antibacterial rate could reach 94.2%, which is excellent compared with other reports.[35–37]

The antibacterial mechanism of Cu^{2+} ions is attributed to the fact that Cu^{2+} ions can combine with the plasma membrane by electrostatic attraction, then penetrate through the plasma membrane and combine strongly with intracellular amino acids and proteases, resulting in the degeneration of this intracellular matter and ultimately the denaturation of proteins.[38,39] Other studies in the literature had similar explanations.[40–42]

Filtration

To investigate the filtration performance of the prepared $(PEI/PSS(Cu)_{1/2})_5$ LBL membranes, Na_2SO_4, NaCl, $MgSO_4$ and $MgCl_2$ each with a concentration of 2000 mg L^{-1} in a single solution were used. The rejection and flux are shown in Table 3.

As can be seen, the rejection by the $(PEI/PSS(Cu)_{1/2})_5$ membrane of 2–2 valent salt $MgSO_4$ was higher than that of 1–1 valent salt NaCl. This is due to the fact that higher ionic valence results in stronger electrostatic repulsion between ions and membrane surfaces with like charge, hence the membrane will have a higher rejection of higher valent ions having like charge. Similarly, the membrane will have a lower rejection of higher valent ions having opposite charge. Therefore, the attraction interaction between ions and those membrane surfaces with opposite charge can be figured out. As shown in Table 3, the rejection of $MgCl_2$ was very low, and that of Na_2SO_4 was high, which demonstrated that the surface of the prepared LBL membrane was negatively charged.

Swelling

Hydrophilic PEs could swell after being immersed in aqueous solution, which could affect the performance of the membrane. So we investigated the stability of the $(PEI/PSS(Cu)_{1/2})_5$ membrane *via* testing the rejection of the same group of LBL membrane samples for Na_2SO_4 and NaCl solutions before and after immersion in DI water for 10 days. The results are shown in Fig. 12.

From Fig. 12 we can see that the rejection and the permeation flux had only slight fluctuations during the testing days. This indicated that the soak time in DI water did not affect the separation performance of the prepared $(PEI/PSS(Cu)_{1/2})_5$ membrane and it had good stability and could be preserved for a long time in water.

Glutaraldehyde post-processing

The uncoordinated amino groups of the prepared LBL NF membranes were subjected to GA crosslinking and the result of the separation performance is shown in Table 4.

As can be seen, the rejection showed an increasing trend, from 84% to 90% after GA post-processing, while the permeation flux showed a decreasing trend, from 65 to 53 L m^{-2} h^{-1}, which demonstrated the occurrence of crosslinking.

The effect of crosslinking on the membrane morphology was also investigated. The SEM images of the LBL membrane before and after GA crosslinking are shown in Fig. 13. It can be seen that the membrane surface became rougher and denser after GA crosslinking.

Conclusions

An H-PAN/PEI/PSS composite NF multilayer membrane was prepared successfully based on a combination of the LBL method and metal–ligand coordination interaction, with an inorganic salt (NaCl) introduced into the polycationic electrolyte PEI solution to control the charge density, and transition metal Cu^{2+} ions introduced into the PSS solution as coordination agent. The optimal preparation conditions were determined, and the performance of the prepared LBL membrane was investigated. The conclusions are as follows:

(1) Transition metal Cu^{2+} ions can be used as metal–ligand coordination agent to prepare LBL functional NF membranes.

(2) The prepared functional LBL NF membrane has excellent antibacterial rate, which could reach over 94% for a five-bilayer LBL NF membrane.

(3) With optimal preparation conditions, the rejection of the five-bilayer NF membrane for Na_2SO_4 is about 84% and the permeation flux is about 65 L m^{-2} h^{-1}; the rejection for NaCl is about 23% and the permeation flux is about 80 L m^{-2} h^{-1}, which means this is a promising membrane for the separation of monovalent and divalent anions.

(4) The prepared functional LBL NF membrane with $PSS(Cu)_{1/2}$ as outmost skin layer shows very good hydrophilicity, with a contact angle maintaining at 15–20°.

(5) Glutaraldehyde crosslinking could further improve the rejection of the prepared LBL NF membrane, while slightly decreasing the permeation flux.

Acknowledgements

We gratefully acknowledge financial support from National Natural Science Foundation of China (No. 20976170, 21476218). This is MCTL Contribution No. 100.

Notes and references

1 G. Decher, *Science*, 1997, **277**, 1232–1237.
2 X. Shi, M. Shen and H. Möhwald, *Prog. Polym. Sci.*, 2004, **29**, 987–1019.
3 G. Decher and J. Hong, *Ber. Bunsen-Ges.*, 1991, **95**, 1430–1434.
4 H. Y. Deng, Q. C. Chen, Z. G. Le, B. K. Zhu and Y. Y. Xu, *Appl. Mech. Mater.*, 2013, **302**, 204–211.
5 Q. Zhao, J. Qian, Q. An and Z. Sun, *J. Membr. Sci.*, 2010, **346**, 335–343.

6 G. Liu, D. M. Dotzauer and M. L. Bruening, *J. Membr. Sci.*, 2010, **354**, 198–205.
7 Z. Wang, B. Su, X. Gao, S. Han and C. Gao, *Mo Kexue Yu Jishu*, 2012, **32**, 27–32.
8 P. Bertrand, A. Jonas, A. Laschewsky and R. Legras, *Macromol. Rapid Commun.*, 2000, **21**, 319–348.
9 H. Lee, L. J. Kepley, H. G. Hong, S. Akhter and T. E. Mallouk, *J. Phys. Chem.*, 1988, **92**, 2597–2601.
10 H. Xiong, Z. Zhou, Z. Wang, X. Zhang and J. Shen, *Supramol. Sci.*, 1998, **5**, 623–626.
11 C. R. South and M. Weck, *Langmuir*, 2008, **24**, 7506–7511.
12 M. Greenstein, R. Ben Ishay, B. M. Maoz, H. Leader, A. Vaskevich and I. Rubinstein, *Langmuir*, 2010, **26**, 7277–7284.
13 G. Zhang, Z. Ruan, S. Ji and Z. Liu, *Langmuir*, 2009, **26**, 4782–4789.
14 Y. Yan and J. Huang, *Coord. Chem. Rev.*, 2010, **254**, 1072–1080.
15 J. Brassinne, C. Mugemana, P. Guillet, O. Bertrand, D. Auhl, C. Bailly, C.-A. Fustin and J.-F. Gohy, *Soft Matter*, 2012, **8**, 4501–4508.
16 V. Marin, E. Holder, R. Hoogenboom and U. S. Schubert, *Chem. Soc. Rev.*, 2007, **36**, 618–635.
17 F. S. Han, M. Higuchi and D. G. Kurth, *Adv. Mater.*, 2007, **19**, 3928–3931.
18 M. Valodkar, S. Modi, A. Pal and S. Thakore, *Mater. Res. Bull.*, 2011, **46**, 384–389.
19 W.-f. Zhang, X.-q. Yan, Z.-h. Wang, L. Sun, Y.-b. Zhao and Z.-j. Zhang, *Gongneng Cailiao*, 2013, **44**, 2156–2161.
20 J. Xu, X. Feng, P. Chen and C. Gao, *J. Membr. Sci.*, 2012, **413–414**, 62–69.
21 J.-h. Fang, Z.-y. Cao, T.-m. Lai and L.-y. Shi, *Gongneng Gaofenzi Xuebao*, 2008, **21**, 218–222.
22 H. Zhang, J. Dang, X. Bai, Y. Shen, Y. Zhang, B. Zhang, Y. Zhang, X. Zhang and J. Liu, *China Pat.*, CN101856596A, 2010.
23 S. Goh, S. Lee, X. Zhou and K. Tan, *Macromolecules*, 1998, **31**, 4260–4264.
24 Z. Han, Y. Wang and J. Wu, *Solid State Sci.*, 2011, **13**, 1560–1566.
25 M. Chanda and G. Rempel, *React. Polym.*, 1995, **25**, 25–36.
26 M. Guittet, J. Crocombette and M. Gautier-Soyer, *Phys. Rev. B: Condens. Matter Mater. Phys.*, 2001, **63**, 125117.
27 W. Bisset, H. Jacobs, N. Koshti, P. Stark and A. Gopalan, *React. Funct. Polym.*, 2003, **55**, 109–119.
28 M. Chen, L. Deng, X. Li and K. Huang, *Guocheng Gongcheng Xuebao*, 2001, **1**, 218–224.
29 S. Kobayashi, K. Hiroishi, M. Tokunoh and T. Saegusa, *Macromolecules*, 1987, **20**, 1496–1500.
30 S. Sun and A. Wang, *J. Hazard. Mater.*, 2006, **131**, 103–111.
31 H. Thiele and K. H. Gronan, *Makromol. Chem.*, 1963, **59**, 207–221.
32 M. Elzbieciak, S. Zapotoczny, P. Nowak, R. Krastev, M. Nowakowska and P. Warszynski, *Langmuir*, 2009, **25**, 3255–3259.
33 B. Su, T. Wang, Z. Wang, X. Gao and C. Gao, *J. Membr. Sci.*, 2012, **423–424**, 324–331.
34 E. M. Vrijenhoek, S. Hong and M. Elimelech, *J. Membr. Sci.*, 2001, **188**, 115–128.
35 L. Yu, Y. Zhang, B. Zhang, J. Liu, H. Zhang and C. Song, *J. Membr. Sci.*, 2013, **447**, 452–462.
36 H. Yu, X. Zhang, Y. Zhang, J. Liu and H. Zhang, *Desalination*, 2013, **326**, 69–76.
37 P. K. S. Mural, A. Banerjee, M. S. Rana, A. Shukla, B. Padmanabhan, S. Bhadra, G. Madras and S. Bose, *J. Mater. Chem. A*, 2014, **2**, 17635–17648.
38 G. Tong, M. Yulong, G. Peng and X. Zirong, *Vet. Microbiol.*, 2005, **105**, 113–122.
39 M. Raffi, S. Mehrwan, T. M. Bhatti, J. I. Akhter, A. Hameed, W. Yawar and M. M. ul Hasan, *Ann. Microbiol.*, 2010, **60**, 75–80.
40 Z. Dan, H. Ni, B. Xu, J. Xiong and P. Xiong, *Thin Solid Films*, 2005, **492**, 93–100.
41 C.-H. Hu and M.-S. Xia, *Appl. Clay Sci.*, 2006, **31**, 180–184.
42 T. Liu, H. Tang, X. Zhang, J. Zhao, R. Cui and X. Sun, *J. Vac. Sci. Technol.*, 2007, **27**, 286–289, 295.

